A FAST SPATIAL DOMAIN METHOD FOR THE SUPPRESSION OF EXCITATION-INDUCED SPURIOUS MODES IN SCN-TLM

S. Lindenmeier[1], B. Isele[2], R. Weigel[2], P. Russer[2]

[1] Ferdinand-Braun-Institut für Höchstfrequenztechnik
Rudower Chaussee 5, D-12489 Berlin, Germany
[2] Technische Universität München, Lehrstuhl für Hochfrequenztechnik
Arcisstr. 21, D-80333 München, Germany

ABSTRACT

A fast method for the suppression of excitation-induced spurious modes in the Transmission Line Matrix (TLM) method is presented for the symmetrical condensed node (SCN) scheme. The method of spurious-free excitation allows for a coarser mesh discretization improving the effectiveness of the TLM-simulation. The capability of the method is demonstrated by way of an example.

INTRODUCTION

In the TLM-method, the electromagnetic field is modeled by a mesh of interconnected transmission lines. We consider symmetrical condensed nodes introduced by Johns [1], which were generalized for lossy media by Nailor und Desai [2], and which became the most popular type of node. Due to the anisotropic propagation characteristic also unphysical *spurious modes* are excited [3]-[5]. Recently, improvements for the excitation of TLM meshes have been reported [6]. Starting with an initial guess of the transversal field distribution, templates for the temporal excitation can be derived by processing of the field components in the ***k***-*ω*-domain thus removing all spurious portions. A key component within this procedure is the adequate mapping between field components and wave amplitudes. In the present work, an improvement to this method is given, rejecting the excitation of *spurious modes* efficiently. The computational effort is reduced to two independent transformations with respect to the longitudinal wavenumber k_z and ω. For weakly dispersive propagation the computational effort can be reduced further to a single temporal transformation. While the mapping of the electromagnetic field components onto the wave amplitudes at the stubs a_{13-18} can be performed according to [1], we have to find a new mapping for the wave amplitudes a_{1-12} at the interconnecting ports. Based on the scattering and propagation processes at the TLM nodes we establish an eigenvalue problem which covers the coupling between the wave amplitudes a_{1-12} and the wave amplitudes a_{13-18} at the adjacent nodes. From coupling between the forward scattered waves and the backward scattered waves within the templates by the transversal boundary conditions, the components of the wave amplitude vector a_{1-12} are determined recursively.

THEORY

The basic TLM algorithm can be written in the ***k***-*ω*-domain as

$$T(\omega)\cdot \boldsymbol{B}(\boldsymbol{k},\omega) = [S]_{18\times18}\cdot A(\boldsymbol{k},\omega) \qquad (1)$$

$$A(\boldsymbol{k},\omega) = [C(\boldsymbol{k})]_{18\times18}\cdot \boldsymbol{B}(\boldsymbol{k},\omega) \qquad (2)$$

The time and space shift in Eqn. (1,2) results in the time- and space shift operators *T,X,Y,Z*, which can be combined in the matrix **C**(***k***). By eliminating the unknown wave amplitude vector **B** and by the help of some addditional basic matrix operations an eigenvalue problem is established which separates the characteristics of the *physical modes* and the unphysical *spurious modes*. We introduce the system matrix ***K*** of the eigenvalue problem

$$[\mathbf{K}]_{18\times18}\cdot\mathbf{A} = \begin{pmatrix} [\mathbf{K}_s]_{12\times12} & [\mathbf{K}_q]_{12\times6} \\ [0]_{6\times12} & [\mathbf{K}_p]_{6\times6} \end{pmatrix}\cdot\begin{pmatrix} \mathbf{A}_{1-12} \\ \mathbf{A}_{13-18} \end{pmatrix} = 0 \qquad (3)$$

The trace matrix K_s relates to the propagation characteristics of the *spurious modes*. The condition

0-7803-3246-6/96/$5.00 © IEEE

1996 IEEE MTT-S Digest

$det(\boldsymbol{K}_s) = 0$ yields six eigenvalues, according to the propagation characteristics of the six different *spurious modes* . These modes are propagating along the main axis of the TLM mesh with twice the speed of light, elucidating their unphysical behavior. The propagation is accompanied by an alternation in sign at every time step. By solving the eigenvalue problem given in Eq. (3) a certain ratio of the wave amplitudes at the interconnecting ports to the wave amplitudes at the stubs is found, for which spurios modes are prevented. The submatrix $\boldsymbol{K}_q$ represents the coupling between the two sets of wave amplitudes $A_{1\text{-}12}$ and $A_{13\text{-}18}$ and implies appropriate mapping rules. A *spurious mode*-free-excitation template representing all wave amplitudes $a_{1\text{-}18}$ at a plane perpendicular to the wave propagation is required for the accurate modeling of planar structures. We consider waveguide structures with the propagation in z-direction and excitation templates that are distributed in a plane perpendicular to the direction of propagation. As is depicted in [6], the *spurious modes* are caused by portions of the amplitudes $a_{1\text{-}12,}$ which do not fulfill the physical relation between the interconnected wave amplitudes $a_{1\text{-}12}$ and the amplitudes at the stubs $a_{13\text{-}18}$.

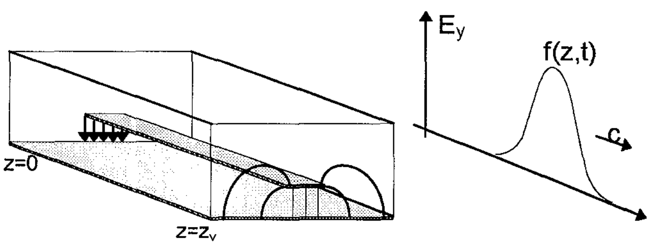

Fig. 1: *Waveguide section with fine discretization for the computation of the preliminary field distribution. Unphysical temporal Gaussian excitation at position z=0, improved field distribution at* $z=z_v$

In a pre-processing step, we apply a fine discretization to a test section with the same cross section as the input section of the structure under investigation. This test section is excited in a conventional way. After the distance $z=z_v$, a field template is extracted for the further processing. Also the propagation velocity *c* in the actual waveguide is measured. Passing the test section the field evolves itself and approaches more and more to the correct field distribution (Fig. 1). The field template is taken when the incident pulse at the position $z=z_v$ reaches its maximum. In a first step, a conventional mapping is applied to the wave amplitudes at the stubs $a_{13\text{-}18}(x,y)$. The template consists of $n_x \times n_y$ nodes. Due to the dispersion relation, which admits propagating modes at $k_x\Delta x=\pi$, $k_y\Delta y=\pi$ in the **k**-space, additional *spurious modes* occur with a spatially alternating sign. However, if a sufficient fine discretization and local low-pass filtering is applied, their influence can be minimized. This results in a nearly *spurious mode*-free field template. For the generation of the amplitudes $a_{9\text{-}12}$, associated with the direction of propagation from the amplitudes at the stubs $a_{13\text{-}18}$, we apply a mapping in the $\boldsymbol{k}$-ω-domain. For example, the amplitude a_9 is given with respect to the transversal coordinates x and y by

$$A_9(x,y,k_z,\omega) = \frac{(1+T)}{(1+TZ)}\left(A_{13}(x,y,k_z,\omega) + \frac{A_{17}(x,y,k_z,\omega)}{Z_y}\right) = \frac{(1+T)}{(1+TZ)}\underline{\Psi}_9(x,y,k_z,\omega) \tag{4}$$

We introduce the amplitude function $\hat{\Psi}$, which is also dependent on the transversal coordinates x and y,

$$\Psi_9(x,y,z,t) = \left(\hat{a}_{13}(x,y) + \frac{\hat{a}_{17}(x,y)}{Z_y}\right) f(z,t) = \hat{\Psi}_9(x,y) f(z,t) \tag{5}$$

Due to the fact that $f(z,t)$ describes the propagation of a pulse in z-direction with the constant velocity *c*, all dependencies from ω and k_z are combined in the function $\underline{\phi}_z(\omega, k_z)$. With Eq. (5) we get the function $\phi_z(z,t)$

$$\Phi_{z9}(z,t) \;\circ\!\!-\!\!\bullet\; \Phi_{z9}(z,\omega) = \frac{1+e^{j\omega\Delta t}}{1+e^{j\omega(\Delta t+\Delta z/c)}}\underline{f}(z=0,\omega)e^{-j\omega z/c} \tag{6}$$

Therefore we have to perform only one a single Fourier transform for each temporal excitation function. Afterwards we apply the function $\phi_z(z,t)$ for obtaining the amplitudes a_9 in the cross section under consideration

$$a_9(x,y,z,t) = \hat{\Psi}_9(x,y)\; \Phi_{z9}(z,t) \tag{7}$$

The amplitudes $a_{10\text{-}12}$ are derived in an analogous way. For the generation of the amplitudes $a_{1\text{-}8}$, directed perpendicular to the propagating direction, lines of nodes within the template are considered. The templates have to be terminated transversally by boundary conditions. The amplitudes along one line of nodes are coupled with each other according to the boundary conditions at the transversal bounds of the template. For the amplitudes a_{1-4} we must consider rows in x-direction, for a_{4-8} we must consider rows in y-direction. The wave amplitudes are evolved pairwise. In Fig. 2, the generation of the amplitudes a_1 and a_2 from the stub values a_{14} und a_{18} is illustrated.

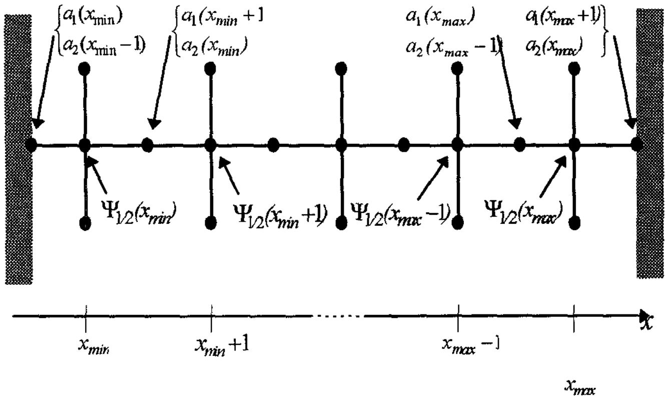

Fig. 2: *Position of the variables within one line of nodes enclosed by boundary conditions in x-direction.*

The following relations in the *k-ω*-domain can be found for the amplitudes:

$$A_{1,2} = \frac{(1+T)}{\left(1+TX^{\pm 1}\right)}\left(A_{14} \pm A_{18}/Z_z\right) \quad \Rightarrow \tag{8}$$

$$\left(X^{\pm 1}\right)A_{1,2} = (1+1/T)(A_{14} \pm A_{18}/Z_z) - (1/T)A_{1,2}$$

This can be expressed in the space domain by

$$\underline{a}_{1,2},(x \pm 1, y, z, \omega) =$$

$$(1+1/T)\left(\underline{a}_{14}(x,y,z,\omega) \pm \underline{a}_{18}(x,y,z,\omega)/Z_z\right) - (1/T)\underline{a}_{2,1}(x,y,z,\omega) \tag{9}$$

The position of the variables is explained in Fig. 2. In the following, we restrict our considerations to dependencies with respect to x and t. The dependencies with respect to the y-axis have to be considered in an analogous way. From Eq. (9) a relation between all a_1 and a_2 along a line of nodes beginning with the given wave amplitudes $a_1(x_{min})$ und $a_2(x_{max})$ closest to the boundary is found, yielding a recursive algorithm for the calculation of wave amplitudes within the template. In the case of quasi-TEM propagation of the pulse the amplitudes at the stubs a_{14} and a_{18} may be separated again into a time function *f(t)* and an amplitude function $\hat{a}$(x). We introduce the function $\hat{\Psi}$(x,y), describing the dependence of the amplitudes to the transversal position x and y. After the determination of the function *ϕ(t)* by expansion of the time function *f(t)* in the frequency domain, the wave amplitudes $a_1(x_{min}, t)$, and $a_2(x_{max}, t)$ closest to the boundary of the template are obtained. The amplitudes a_1 and a_2 on the row are calculated from starting values at x_{min} and x_{max} also in time and space domain. The remaining amplitudes a_{3-8} can be calculated in an analogeous way according to the mapping given by Eq. (8). The computational effort is kept low, since each transformation is necessary only once for the same type of transversal situation.

NUMERICAL EXAMPLE

We verify our method by the simulation of a coplanar waveguide (CPW) section. The structure was discretized in a coarse mesh 14×7 cells in the cross section, emphasizing the occurance of *spurious modes* in the conventional excitation. For the extraction of the test section we apply a Gaussian pulse with time window t_{max}=60Δt and period t_0=13.3Δt. The processing of the wave amplitudes within the template yields the time functions Φ_z, which are depicted in Fig. 3. These functions describe modifications made to the wave amplitudes for the rejection of *spurious modes*.

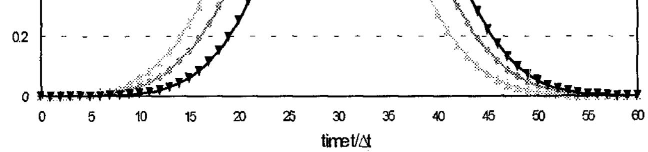

Fig. 3: *Time histories Φ_z of the excitation of wave amplitudes in propagation direction with Gaussian shape and suppressed spurious mode.*

The time functions representing the wave amplitudes a_9 and a_{11}, which are associated with the positive direction of propagation, hurry ahead the Gaussian pulse, whereas the function representing the wave amplitudes a_{10} and a_{12}, which are associated with negative direction of propagation, lag the original Gaussian pulse. The shapes and amplitudes of these functions were mutually changed, too. The functions $\phi_{x,y}(t)$, describing the modifications of wave amplitudes perpendicular to the direction of propagation are shown in Fig. 4. Depending on the boundary conditions on each side these functions may have totally different shape. In Fig 5. three methods are compared: Curve 1 shows the impulse response to Gaussian excitation, after passing a waveguide section.

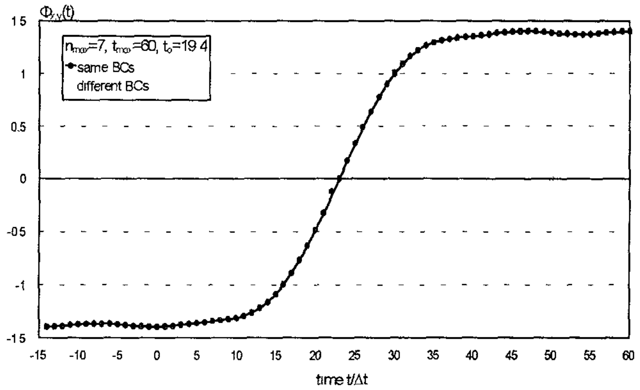

Fig. 4: *Time histories $\Phi_{x,y}$ for the wave amplitudes associated with the x- and y-direction for same and different boundary conditions (BC) on each side*

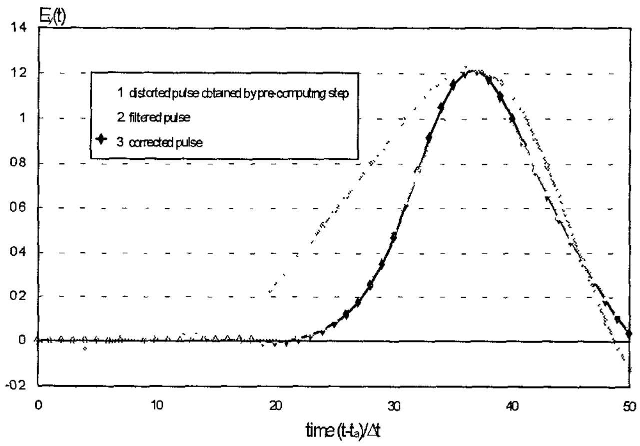

Fig 5: *Impulse responses to Gaussian excitation for different methods.*

Due to dispersion effects [3],[6] in a coplanar waveguide and the additional dispersion introduced by the TLM mesh the pulse becomes distorted. However, when the passing pulse reaches its maximum useful field templates can be extracted, which approach the physical field distribution. Nevertheless *spurious modes* are visible in the signal. They are generated by an unphysical excitation of the waveguide section and gain more influence at the discontinuities of the circuit. Conventional mapping causes the excitation of *spurious modes*. Therefore the time response is distorted as depicted by curve 2. Using our new approach for the mapping between field components and wave amplitudes, the occurence of spurious modes is suppressed as is demonstrated by curve 3.

CONCLUSION

We present a method for the suppression of spurious modes in the excitation of TLM meshes. The feasibility of the approach is demonstrated by way of an coplanar line section, which was fed by a Gaussian pulse at one port. We found a complete suppression of *spurious modes* using the new method, which also fulfills the energy conservation condition exactly.

References

[1] P.B. Johns, „A symmetrical condensed node for the TLM method," *IEEE Trans. Microwave Theory Tech.* MTT-35, pp. 370-377, April 1987

[2] P. Naylor, R.A. Desai, „New three dimensional symmetrical condensed lossy node for solution of electromagnetic wave problems by TLM," *Electron. Lett.*, Vol. 26, pp. 492-495, March 1990

[3] W. Schroeder, I. Wolff, „The origin of spurious modes in numerical solutions of electromagnetic field eigenvalue problems," *IEEE Trans. Microwave Theory Tech.* MTT-42, pp. 644-653, April 1994

[4] N. Schulz, K. Bierwirth, F. Arndt, U. Koester, „Finite difference method without spurious solutions for the hybrid analysis of diffused channel waveguides," *IEEE Trans. Microwave Theory Tech.* MTT-38, pp. 722-729, June 1990

[5] J.S. Nielsen, „Spurious modes of the TLM condensed node formulation," *IEEE Microwave Guided Lett.*, Vol. 1, pp. 201-203, August 1991

[6] S. Lindenmeier, B. Isele, R. Weigel, P. Russer, „Improved initial conditions for the symmetrical condensed TLM-node with respect to physical propagation characteristics," Proc. *Progress in Electromagnetics Research Symposium (PIERS)*, Noordwijk, The Netherlands, CD-ROM (4 pages), July 1994